

# TEST OF A PROTOTYPE FOR MODULAR PROFILE AND POSITION MONITORS IN THE SHIELDING OF THE 590 MeV BEAM LINE AT HIPA

R. Dölling<sup>†</sup>, M. Sapinski, F. Marcellini, Paul Scherrer Institut, Villigen, Switzerland

## Abstract

A new generation of monitor plugs is under development as spares for the ageing wire profile monitors and beam position monitors inserted into massive shielding in the target regions of the 590 MeV proton beam line at HIPA. A prototype was installed recently in the beam line to the ultra-cold neutron source UCN, to test the performance of wire monitor, BPM and modular mechanical design in a low-radiation environment. We report on first measurements with beam.

## INTRODUCTION

The design of the prototype [1, 2] and its vacuum chamber closely resembles the one foreseen in the target region, just the intermediate section with the shielding is subtracted. Beam to UCN is provided either continuously as a splitted beam of a few  $\mu\text{A}$  or as the full deflected 1800  $\mu\text{A}$  beam for 8 s, repeated every 300 s.

## WIRE MONITOR

At the location of the prototype, the vertical width of the beam is narrow, resulting in the highest thermal load to a wire monitor in the 590 MeV beam lines. The load is higher at the horizontally moving wires MBPT1 than at the vertically moving wires MBPT2. In addition, the wire speed of the prototype is actually only 0.06 m/s, four times lower than that of most in-shielding monitors. This is due to the maximum rate of full steps of 2 kHz, which can be provided by the actual MESON modules [3] driving the stepper motor and reading the signal currents from the wires. The speed will be increased at a later step, when the new driver electronics, based on an extension of the read-out electronics [2] under development, is available. To compensate for the low speed, we reduced the diameter of the molybdenum wires from 48  $\mu\text{m}$  to 25  $\mu\text{m}$  in a first step. In a second step we reduced the diameter to 13  $\mu\text{m}$  and the number of wires per monitor from two to one. In each scan the wires of horizontal and vertical monitor synchronously pass the beam with a forward and a backward motion, ‘meeting’ at the beam axis twice. Each scan is documented by the control software.

## Wire Performance

Secondary emission (SE) as well as thermionic emission (TE) can contribute to the wire signal. Unlike [4], we did not bias the wires to a positive potential for suppressing TE. With the 25  $\mu\text{m}$  wires we observed an evolution of TE over a few passes with higher beam current applied (Figs. 1-4).

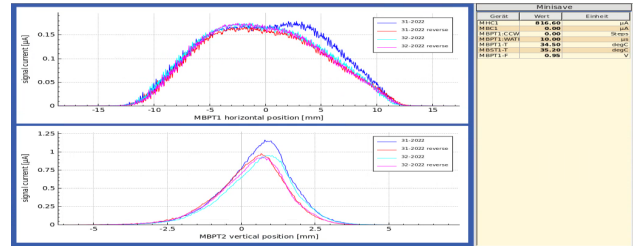


Figure 1: Two scans at a beam current of 820  $\mu\text{A}$  (first time above 100  $\mu\text{A}$ ). In the first pass, a TE contribution is visible at MBPT1, but in the following three passes not. (The beam current was stable during this time.) A single pass at 820  $\mu\text{A}$  seems sufficient to ‘condition’ the surface for lower TE.

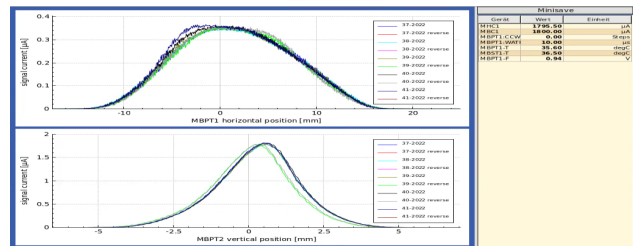


Figure 2: After five further scans with beam current increased to 1800  $\mu\text{A}$ , first signs of TE appeared at MBPT1.

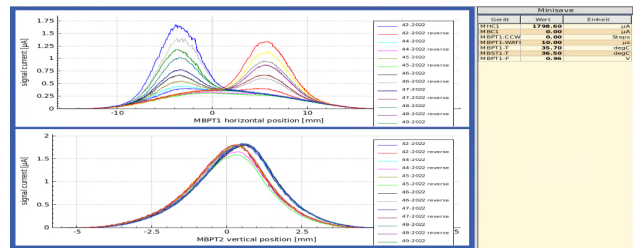


Figure 3: In the following 9 runs at 1800  $\mu\text{A}$ , TE reappeared strongly at MBPT1 in the second half of the passes, where the wire has already heated up. However, the signal without TE, visible in the first half of the passes, does not change much. This indicates that the wire diameter is not reduced due to evaporation.

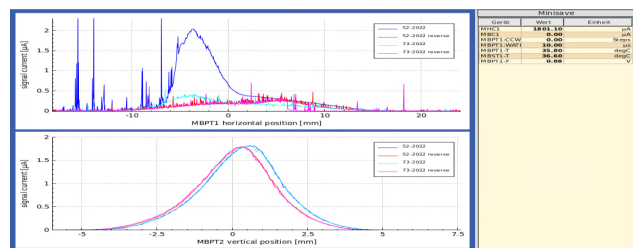


Figure 4: In the next scan, the 21<sup>st</sup> with beam current above 800  $\mu\text{A}$ , the first of the horizontally moving wires (MBPT1) broke. This resulted in increased noise from the dangling wire ends. In the 39<sup>th</sup> scan, the second horizontally moving wire also broke.

<sup>†</sup> doelling@protonmail.com

Content from this work may be used under the terms of the CC BY 4.0 licence (© 2021). Any distribution of this work must maintain attribution to the author(s), title of the work, publisher, and DOI

At the presence of TE at MBPT1, also a small increase of signal at MBPT2 is visible (Figs. 1-3), however nearly independent of the amount of TE at MBPT1.

The increase of TE over the series of scans may be caused by a change of work function or by a lower emissivity leading to higher maximum temperatures. The latter is more likely, since the wire breakage hints to the presence of higher temperatures. A simulation of the heating (Fig. 5) indicates that at full beam current evaporation of wire material should be significant. A lifetime of 29 scans is predicted by that. This is contradicting the conclusion from Fig. 3 and the microscopic observation of the wire end (Fig. 6). Further studies are needed to get a better understanding.

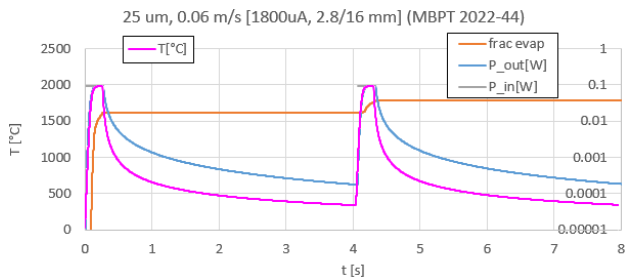


Figure 5: Rough simulation of 25  $\mu\text{m}$  wire heating in the beam center at 1800  $\mu\text{A}$  beam current. Wire temperature, fraction of evaporated material, input and output power are calculated assuming a homogeneous rectangular beam with width double the fwhm measured, stopping power @590 MeV, specific heat @1000°C and temperature dependent emissivity and evaporation rate given by [5]. Thermal equilibrium is reached after the first half of the pass.



Figure 6: End of broken wire at a magnification of  $\sim 800$ . No thinning is visible.

With the single 13  $\mu\text{m}$  wire, the signal is lower in accordance with the reduced sum of wire circumferences. Signal to noise ratio in the beam core is comparable. A very minor TE contribution appeared only at the first scan at 200  $\mu\text{A}$  beam. However the application of beam currents of up to 2000  $\mu\text{A}$  caused a relative decrease of signal at later scans at low beam current. We still have to accumulate a larger number of scans to see a development. A simulation analogous to Fig. 5 predicts  $\sim 450^\circ\text{C}$  lower temperatures for the thinner wire and an evaporation-related lifetime of 20000 scans. Thermal equilibrium is still reached and a wire speed above 0.24 m/s would be required to lower temperatures. According to simulation, the 48  $\mu\text{m}$  wires of the other 590 MeV monitors survive only due to lower beam current densities in that locations.

### Force Sensor

A force sensor allows to observe the force applied to the feedthrough and in-vacuum mechanics. It performs well in spite of a long cable length of  $\sim 30$  m (Fig. 7).

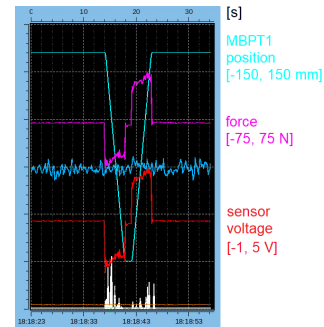


Figure 7: Force sensor reading at full scan. The force at rest corresponds to the weight of the moved parts.

### BPM

The capacitive pickup variant (Ref. [2] Fig. 6, modified for horizontal beam) has been implemented in the prototype. The signals of the four pickups are transferred via a short radiation hard (metal, ceramics) cable module and a short PE cable with removed mantle to the feedthrough, and further via  $\sim 30$  m of 1/4"-Cellflex SCF14-50JFN cable with a damping of  $\sim 1.8$  dB to a LeCroy 640zi scope or an Rhode&Schwarz FSV spectrum analyser. Different from the standard BPM, no preamplifier is used in the bunker.

### Higher-Order Modes of the Monitor

With the large diameter and short length of the BPM, and with profile monitor parts nearby, higher-order modes (HOM) excited by the beam are more prominent than in our standard BPMs. In the measured signal spectrum (Fig. 8), this is visible as an increased ‘underground’ at around 300 MHz and above 700 MHz, besides the harmonics of the bunch repetition frequency  $f_{RF} = 50.63$  MHz.

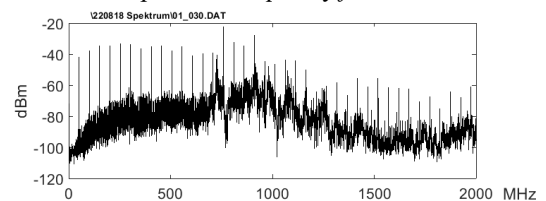


Figure 8: Spectrum of a single pickup at a beam of 1800  $\mu\text{A}$  taken with the spectrum analyser at a bandwidth of 20 kHz.

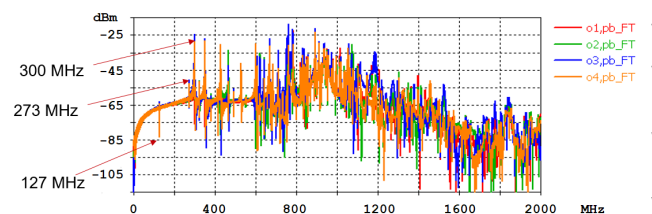


Figure 9: HOM spectrum according to a CST simulation. Excitation by a single bunch of 1800  $\mu\text{C}$  and 58 mm r.m.s. length.

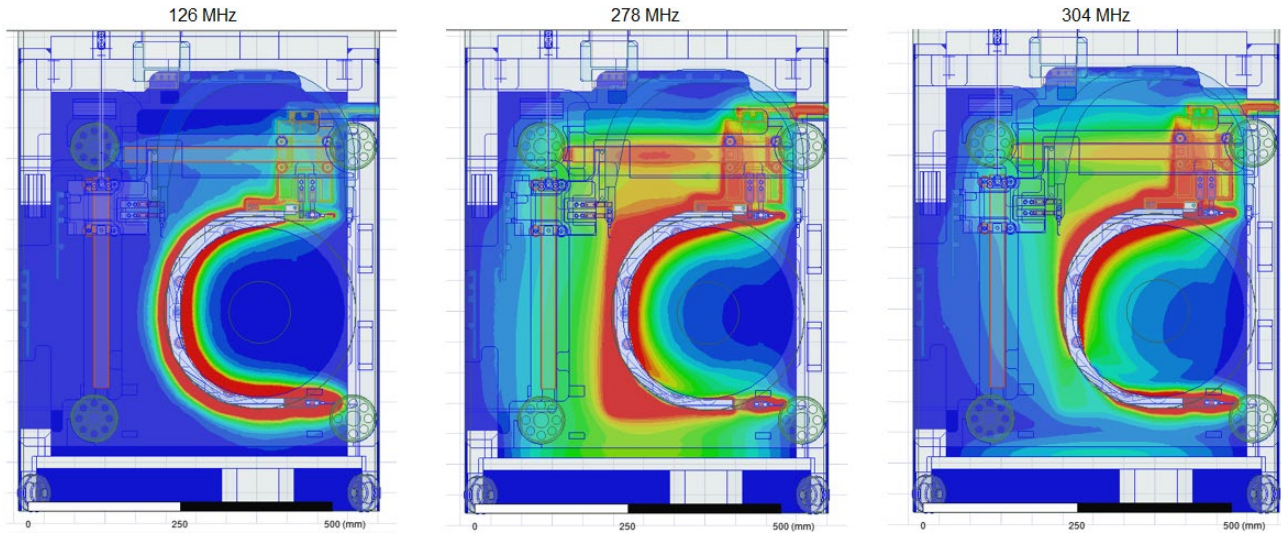


Figure 10: Distribution of electric field of the first three HOM. Structure grounded at chamber bottom and top.

This relates to a detailed CST simulation of the monitor structure (Figs. 9 and 10). The HOM spectra of measurement and simulation compare reasonably. The fork of the horizontally moving MBPT1, which in the parking position is close to the beam, is involved in all three modes. A grounding of the fork's free end in the parking position would shift these HOM to much higher frequencies. However, it is difficult to provide this reliably.

### Position Determination

To measure the signals of all four pickups the 4-channel scope was used. Fig. 11 gives an example.

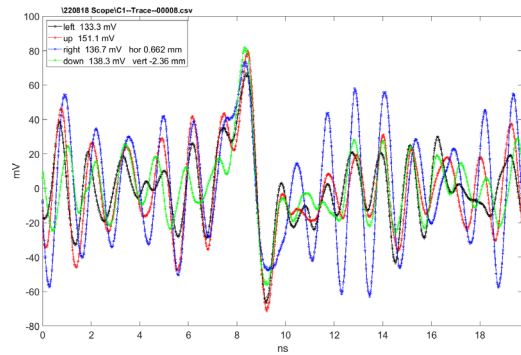


Figure 11: The four pickup signals averaged over 5063 periods of  $f_{RF}$ . Sampling rate 20 GS/s. (The legend gives the peak-to-peak height and the position derived from this by using Eq. (1) with zero offset.)

From a FFT of the pickup signals, the intensities of the first 12 harmonics of  $f_{RF}$  were determined by adding all channels in a peak above 3 per mille of the maximum. This was done for several vertically shifted beams of known vertical position  $y_{ref}$ . The relation

$$y_{BPM}[\text{mm}] = r_{\text{eff}}[\text{mm}] \frac{U_{\text{down}} - U_{\text{up}}}{U_{\text{down}} + U_{\text{up}}} + y_{\text{offset}} \quad (1)$$

could be established with  $r_{\text{eff}} = 53$  mm and significant offsets  $y_{\text{offset}}$ , depending on the used harmonic, which are caused by the presence of HOM (Fig. 12). The CST simulation predicted  $r_{\text{eff}} \sim 55$  mm in good agreement. (The

physical radius of the BPM is 100 mm.) Just for harmonic 2, which is used at our standard BPM, the offset is here close to 0 mm. However, the BPM should be calibrated with the profile monitor. We still have to determine if these offsets depend on beam current.

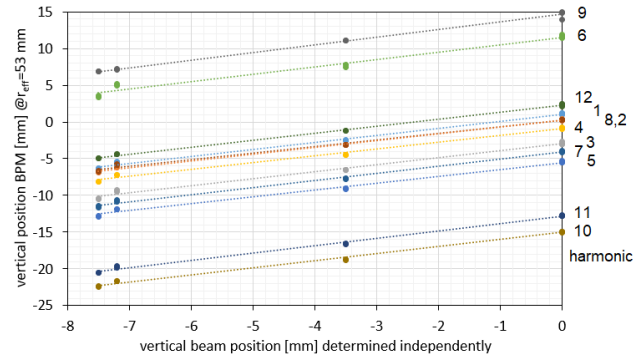


Figure 12: Correlation between vertical beam position measured by MBPT2 and neighbouring BPM with the beam position determined by the BPM prototype. Beam current 1800  $\mu\text{A}$ .

### Subharmonics

Interestingly, subharmonics at multiples of  $f_{RF}/10$  appear in all measured spectra over a broad range (Fig. 13). This frequency is not natural to the RF amplifiers or RF cavities or resonators of both upstream cyclotrons or bunchers. However, in the far upstream Injector 2 cyclotron with a harmonic number of 10,  $f_{RF}/10$  corresponds to the time of a turn revolution, i.e. to the time difference between bunches moving in the same radial 'spoke' of bunches, but at radially neighbouring turns.

Somehow 'information' must be transferred from a bunch in a turn to a bunch in a neighbouring turn, being then 'displaced' by the time of a turn revolution. It is likely that beam current noise at frequencies in the kHz and low MHz range, which is overlaid to the bunch pattern and generated mainly by the ion source, plays a role here. (e.g., a measurement of the number of turns in the cyclotron [6] is based on this.)



A candidate for the transfer of protons may be the beam extraction. The last turns are separated to a high degree at the electrostatic septum, but a small overlap remains. Hence, a small fraction of protons from the second last turn is also extracted. Beam dynamics considerations must clarify if these protons ‘survive’ up to the much downstream location of the BPM.

A candidate for the transfer of information on bunch charge are the strong space charge forces in the Injector 2, which also affect radially neighbouring bunches. There is no indication of the presence of  $f_{RF}/6$  subharmonics corresponding to the Ring cyclotrons harmonic number. However, the space charge forces are lower there.

It would be interesting to clarify the underlying mechanism, since such measurements may possibly deliver information on the quality of extraction, the space charge forces or other parameters.

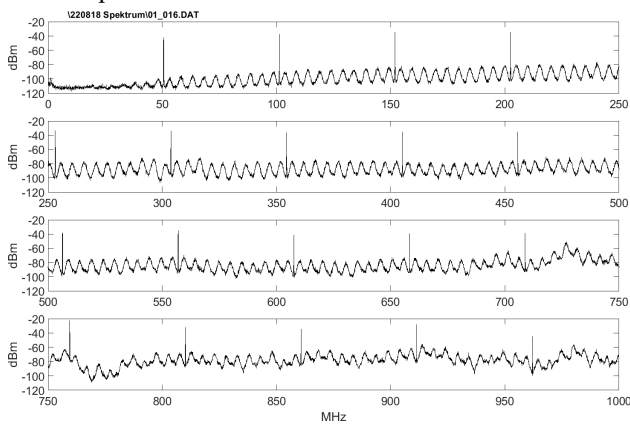


Figure 13: Spectrum of a single pickup at a beam of 1800  $\mu$ A taken with the spectrum analyser at a bandwidth of 2 kHz.

## ACKNOWLEDGEMENTS

The authors would like to thank R. Widmer and S. Lindner for assembling the monitor, T. Rauber and P. Simon for providing vacuum chamber and lifting gear and organizing bunker works, J. Snuvering for adapting the profile monitor driving software, H. Lutz, G. Gamma and K. Bitterli for electronics and controls integration, J.-Y. Raguin for additional RF simulations, B. Keil, A. Dietrich, M. Rizzi, M. Schneider and D. Treyer for discussions.

## AUTHOR CONTRIBUTIONS

RD and MS provided the wire monitor chapter. RD provided the BPM chapter with exception of the CST simulations which were done by FM.

## REFERENCES

- [1] R. Dölling, D. Berisha, J. Germanovic, D. C. Kiselev, F. Marcellini, and K. M. Zehnder, “Development of Modular Spare Parts for the Profile and Position Monitors of the 590 MeV Beam Line at HIPA”, in *Proc. IBIC'19*, Malmö, Sweden, Sept. 2019, pp. 402-406.  
doi:10.18429/JACoW-IBIC2019-TUPP035
- [2] R. Dölling, E. Johansen, M. Roggli, and M. Rohrer, “Progress of Profile Measurement Refurbishment Activities at HIPA”, in *Proc. IBIC'20*, Santos, Brazil, Sep. 2020, pp. 179-183.  
doi:10.18429/JACoW-IBIC2020-WEPP33
- [3] E. Johansen, “VME Meson design specification”, PSI, Villigen, Switzerland, June 2010, unpublished.
- [4] M. Sapinski, R. Dölling, M. Rohrer, “Commissioning of the renewed long radial probe in PSI’s Ring Cyclotron”, presented at IBIC’22, Krakow, Poland, Sept. 2022, poster MOP19, this conference.
- [5] <https://www.plansee.com/de/werkstoffe/molybdaen.html>
- [6] P. A. Duperrex and A. Facchetti, “Number of turn measurements on the HIPA cyclotrons at PSI”, in *Proc. IPAC'18*, Vancouver, Canada, Apr.-May 2018, pp. 2334-2336,  
doi:10.18429/JACoW-IPAC2018-WEPA067